

NANO EXPRESS

Open Access

Magnetic Mn₅Ge₃ nanocrystals embedded in crystalline Ge: a magnet/semiconductor hybrid synthesized by ion implantation

Shengqiang Zhou^{1*}, Wenxu Zhang^{2*}, Artem Shalimov¹, Yutian Wang^{1,3}, Zhisuo Huang², Danilo Buerger¹, Arndt Mücklich¹, Wanli Zhang², Heidemarie Schmidt⁴ and Manfred Helm^{1,3}

Abstract

The integration of ferromagnetic Mn₅Ge₃ with the Ge matrix is promising for spin injection in a silicon-compatible geometry. In this paper, we report the preparation of magnetic Mn₅Ge₃ nanocrystals embedded inside the Ge matrix by Mn ion implantation at elevated temperature. By X-ray diffraction and transmission electron microscopy, we observe crystalline Mn₅Ge₃ with variable size depending on the Mn ion fluence. The electronic structure of Mn in Mn₅Ge₃ nanocrystals is a 3d⁶ configuration, which is the same as that in bulk Mn₅Ge₃. A large positive magnetoresistance has been observed at low temperatures. It can be explained by the conductivity inhomogeneity in the magnetic/semiconductor hybrid system.

Keywords: Mn₅Ge₃, Ion implantation, Magnetic nanocrystals, Magnetoresistance

Background

Due to its compatibility to Si technology, Ge has attracted special attention as a host semiconductor for diluted magnetic impurity atoms. However, due to the low solid solubility of transition metals in Ge, intermetallic compounds (mainly Mn₅Ge₃) tend to form in the Ge host [1-6]. Mn₅Ge₃ is a half metallic ferromagnet with a large spin polarization [7]. By first principle calculation, large spin injection efficiency is expected by the integration of Mn₅Ge₃ within the Ge matrix [7]. Electrical spin injection and detection in Ge have been experimentally demonstrated [8,9]. Therefore, considerable work has been done to fabricate epitaxial Mn₅Ge₃ films as well as nanostructures [10-12]. The Curie temperature (T_C) of Mn₅Ge₃ is 296 K, which can be effectively increased by carbon doping. Spiesser et al. reported the epitaxial growth of Mn₅Ge₃C_x films on Ge (111) [13]. When x is around 0.6, T_C can be as high as 430 K. On the other hand, some unknown nanoscale

Mn-rich phases also form under particular conditions during molecular beam epitaxy (MBE) growth [14-19]. Those nanostructures can have a T_C much higher than 300 K. Besides MBE, ion implantation has been used to prepare ferromagnetic semiconductors as well as hybrids of ferromagnets embedded in semiconductors [20-24]. The advantages of ion implantation include compatibility with conventional Si-chip technology and lateral patterning. Patterning by ion implantation allows the synthesis of magnetic structures comprising different magnetic phases. By carbon implantation into Mn₅Ge₃ and Mn₅Si₃, Sürgers et al. obtained lateral magnetic hybrid structures in the micrometer and submicrometer range [25]. In this contribution, we report the preparation of magnetic Mn₅Ge₃ nanocrystals embedded inside the Ge matrix by Mn ion implantation at an elevated temperature. We identify the formation of nanocrystalline Mn₅Ge₃ by X-ray diffraction (XRD) and transmission electron microscopy (TEM). The magnetic, electronic, and magnetotransport properties will be reported for this magnetic/semiconductor hybrid system.

Methods

Nearly intrinsic Ge(001) wafers (n-type with the electron concentration of 10¹³ to 10¹⁴ cm⁻³) were implanted with

* Correspondence: s.zhou@hzdr.de; xwzhang@uestc.edu.cn

¹Institute of Ion Beam Physics and Materials Research, Helmholtz-Zentrum Dresden-Rossendorf, PO Box 510119, Dresden 01314, Germany

²State Key Laboratory of Electronic Thin Films and Integrated Devices, University of Electronic Science and Technology of China, Chengdu 610054, China

Full list of author information is available at the end of the article

100-keV Mn ions at 673 K to avoid amorphization. It is worthy to note that we also used p-type Ge(001) as the substrates and got similar structural and magnetic properties. We varied the ion fluence to get samples with a large range of Mn concentrations, resulting in different structural and magnetic properties. The corresponding preparation and characterization parameters are listed in Table 1. Structural analysis was performed by synchrotron radiation XRD (SR-XRD) at the Rossendorf beamline (BM20) at the ESRF with an X-ray wavelength of 0.154 nm. Magnetic properties were analyzed using a superconducting quantum interference device magnetometer (Quantum Design Inc., San Diego, CA, USA) with the field along the sample surface. X-ray absorption spectroscopy (XAS) measurements were performed at the beamline UE46/PGM-1 at BESSY II (Helmholtz-Zentrum, Berlin, Germany). Magnetotransport properties were measured using the van der Pauw geometry with a magnetic field applied perpendicular to the film plane. Fields up to 9 T were applied over a wide temperature range from 5 to 300 K.

Results and discussion

Mn₅Ge₃ nanocrystal formation

The SR-XRD 2θ-θ scans confirm the formation of Mn₅Ge₃ nanomagnets. As shown in Figure 1, beside the main peaks from Ge(004), the diffraction peaks of Mn₅Ge₃(111), (002), (310), (222), and (004) are clearly visible. Note that, compared to the work by Ottaviano et al. [20], the SR-XRD reveals more Mn₅Ge₃ peaks even for a much smaller Mn ion fluence due to the large flux of X-rays from the synchrotron source, which allows for the detection of small Mn₅Ge₃ nanocrystals. Therefore, we have to revisit the work by Ottaviano et al. They concluded that Mn₅Ge₃ nanocrystals formed by ion implantation are preferentially (002)-oriented in the Ge (001) matrix [20]. However, Zeng et al. [10] prepared Mn₅Ge₃ layers by molecular beam epitaxy, and they found the crystalline orientation as Mn₅Ge₃(001) || Ge(111). The SR-XRD observations therefore led us to conclude that Mn₅Ge₃ nanocrystals formed by Mn implantation are indeed randomly oriented inside the Ge(001) matrix, which is also supported by the magnetic properties shown later. We found nearly isotropic hysteresis loops with magnetic field along different directions. Note that in the work of Jain et al. [26], the Mn₅Ge₃ nanocrystals were

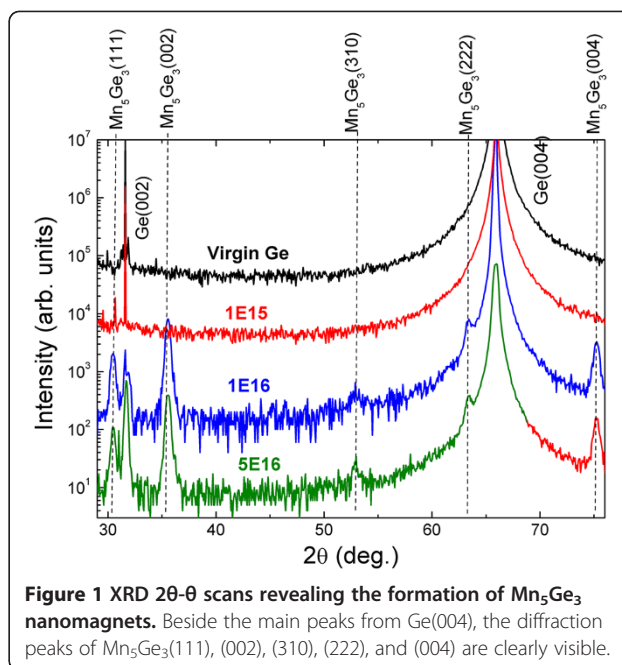


Figure 1 XRD 2θ-θ scans revealing the formation of Mn₅Ge₃ nanomagnets. Beside the main peaks from Ge(004), the diffraction peaks of Mn₅Ge₃(111), (002), (310), (222), and (004) are clearly visible.

grown by annealing GeMn films on Ge(001) substrates prepared by MBE. Most of the Mn₅Ge₃ clusters (97%) have their *c*-axis perpendicular to the film plane. The accumulated literature data suggest that the growth of Mn₅Ge₃ nanocrystals from the Ge matrix is different from the Mn₅Ge₃ thin films.

Figure 2 shows cross-section TEM images of samples 1E16 and 5E16. The white contrast spots are from precipitates that are located in the depth between 20 and 120 nm, which is in agreement with the depth profile of Mn ion implantation. The average crystallite size is increased from 5 to 11 nm with increasing Mn fluences from 1×10^{16} to 5×10^{16} cm⁻². For detailed analysis, we focus on the sample 5E16. As shown in Figure 2b, the well-defined Moiré patterns are a strong indication for monocrystalline precipitates embedded in a crystalline matrix. Using high-resolution TEM, the precipitates can be identified to be Mn₅Ge₃, as shown in Figure 2c,d. Figure 2d is the fast Fourier transform (FFT) of the image shown in Figure 2c. The FFT reveals lattice spacings amounting to 0.298 nm (indicated by the open circles) and 0.623 nm (indicated by the open squares), which correspond to Mn₅Ge₃(111) and (001), respectively.

Table 1 Sample identification, structural, and magnetic parameters

Sample identifier	Mn fluence	Concentration	Mn ₅ Ge ₃ (XRD)	T _{max} (ZFC/FC)	Average diameter
1E15	1×10^{15} cm ⁻²	0.2%	-	-	-
1E16	1×10^{16} cm ⁻²	2%	Yes	185 K	5 nm
5E16	5×10^{16} cm ⁻²	10%	Yes	270 K	11 nm

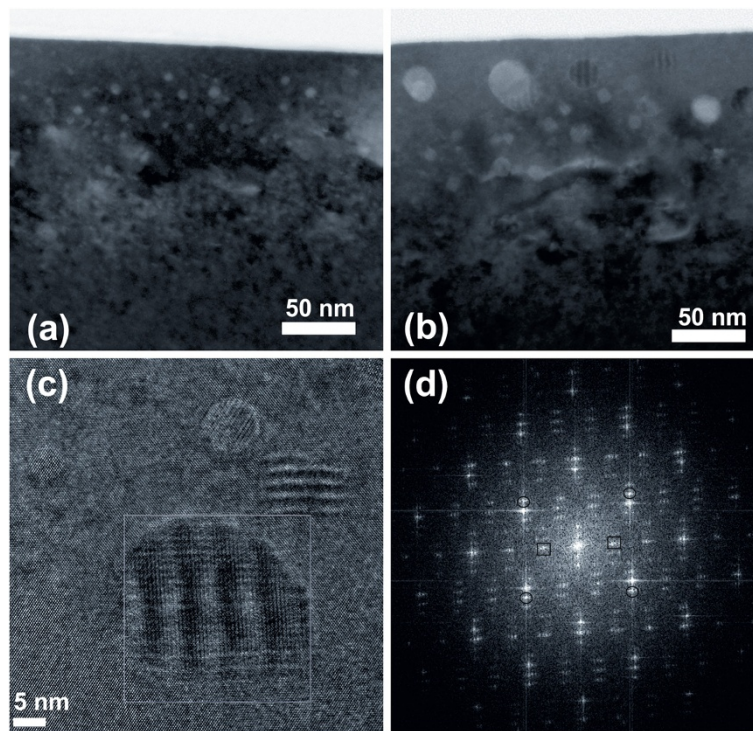


Figure 2 TEM and high-resolution TEM images of samples. TEM image of the cross section showing the formation of precipitates (a) 1E16 and (b) 5E16, and high-resolution TEM for an individual Mn_5Ge_3 particle (c) in sample 5E16. (d) FFT of the precipitate indicated in (c).

Magnetic properties

Figure 3a shows the zero field-cooled and field-cooled (ZFC/FC) magnetization curves in a 50-Oe field for different Mn fluences. The FC curve for sample 1E15 completely overlaps with the corresponding ZFC curve at around zero. Magnetic Mn_5Ge_3 nanocrystals can be excluded in this sample, which is consistent with the SR-XRD observation, except that they are very small and dilute beyond the detection limit of SR-XRD. For samples 1E16 and 5E16, a distinct

difference in the ZFC/FC curves was observed. The ZFC curves show a gradual increase at low temperatures, peaking at different temperatures, while the FC curves monotonically increase with decreasing temperature. The width of the peaks in the ZFC curves is due to the size distribution of Mn_5Ge_3 nanocrystals, as shown in the TEM images (Figure 2). In this paper, we take the temperature (T_{max}) at the maximum of the ZFC curve as the average blocking temperature listed in Table 1.

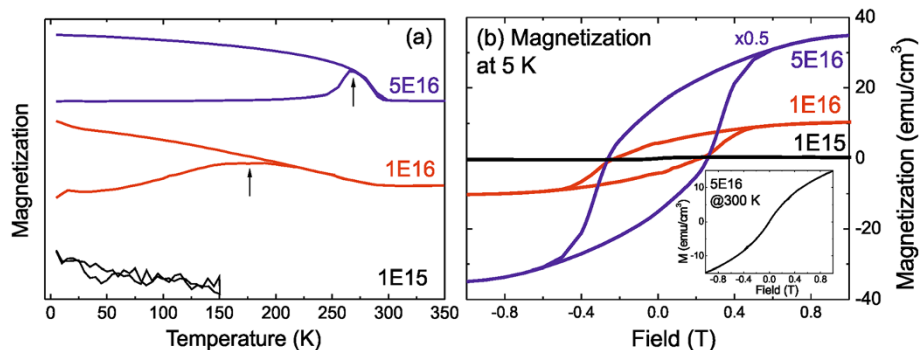


Figure 3 ZFC/FC magnetization and hysteresis loops. (a) Magnetization curves with an applied field of 50 Oe after ZFC/FC for the Mn-implanted Ge. The lower branches are ZFC curves, while the upper branches are FC curves. With increasing fluence, the Mn_5Ge_3 nanocrystals are growing in size, resulting in a higher blocking temperature. The curves are vertically shifted to increase the visibility. (b) Hysteresis loops measured at 5 K for Mn-implanted Ge with different fluence, and the inset shows the magnetization at 300 K for sample 5E16.

Figure 3b shows the magnetization versus field reversal (M-H) of all samples measured at 5 K. Hysteretic behaviors were observed for samples 1E16 and 5E16. With increasing Mn concentration, the saturation magnetization is increased from 10.1 to 69.2 emu/cm³ (by assuming the implanted depth of 100 nm), and the coercivity is increased from 0.22 to 0.26 T. At 300 K, sample 5E16 only shows field-induced magnetization (see the inset of Figure 3b). The saturation magnetization of the sample 5E16 (1E16) is 69.2 (10.1) emu/cm³, corresponding to around 1.5 (1.1) μ_B /Mn, which is smaller than $2.6 \pm 0.5 \mu_B$ /Mn as reported in the study of Bihler et al. [1], which means that not all of the implanted Mn ions form the ferromagnetic Mn₅Ge₃ phase.

We also compared the magnetization between the in-plane and out-of-plane directions at 5 K for sample 5E16 (not shown). In contrast to the studies of Bihler et al. [1] and Jain et al. [8], there is no detectable magnetic anisotropy. For the bulk Mn₅Ge₃, the magnetic easy axis is [001]. The absence of magnetic anisotropy in our samples is due to the random crystallographic orientation of the Mn₅Ge₃ nanocrystals.

As shown in Figure 3b, the hysteresis loop is not square-like. The distribution of coercivity field is due to the size distribution of the nanomagnets, as evidenced by the TEM images, and is also possibly due to the random distribution of the nanomagnet easy axis. According to the Stoner and Wohlfarth model for single-domain magnetic nanoparticles, the maximum coercive field gives the anisotropy field $\mu_0 H_{a2} = 0.26$ T for sample 5E16. Using the bulk saturation magnetization (M_S) for Mn₅Ge₃ (1,100 kA/m) [26], one can deduce the anisotropy constant: $K_2 = \mu_0 H_{a2} M_S / 2 \approx 1.4 \times 10^5$ J/m³, which is smaller than the value reported by Jain et al. [26]. Based on the Néel-Brown model, the volume for a nanomagnet $V = 25k_B T_{\max} / K_2$ (k_B as the Boltzmann constant), we calculate the average diameter of Ge₃Mn₅ clusters in sample 5E16 to be approximately 10.8 nm ($T_{\max} = 270$ K). The average diameter is in good agreement with the results obtained by TEM. However, the average diameter for sample 1E16 deduced from the ZFC magnetization is as large as 9.5 nm, which is much larger than the value from the TEM observation.

The magnetic properties of the Mn-implanted Ge were also investigated by X-ray magnetic circular dichroism (XMCD) at Mn $L_{2,3}$ edge. Right before the XAS measurements, the sample was etched in deionized water for 2 min to remove the surface oxide layer [27]. Figure 4a presents the Mn $L_{2,3}$ XAS measured in total electron yield mode at around 4.5 K; $\mu+$ and $\mu-$ represent the absorption intensity with the direction of magnetization parallel and antiparallel to the photon helicity, respectively. As shown in Figure 4a, after etching, we obtained very similar spectra as was reported for ferromagnetic

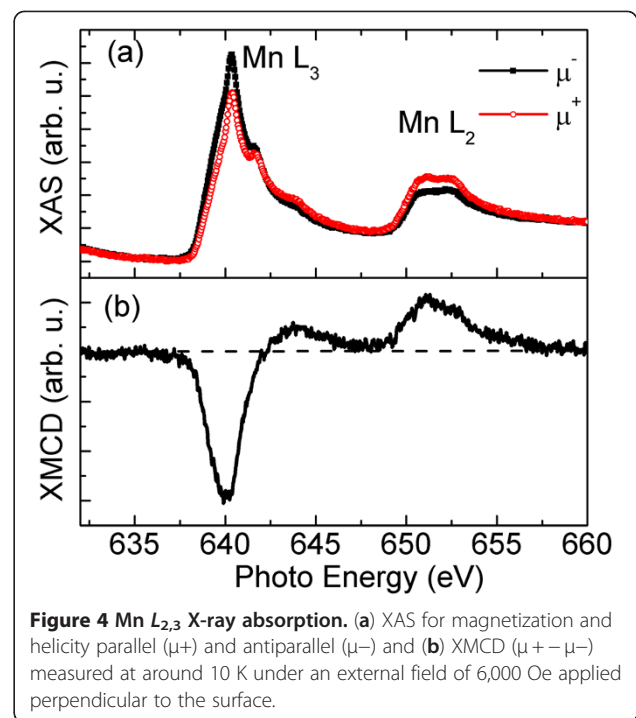
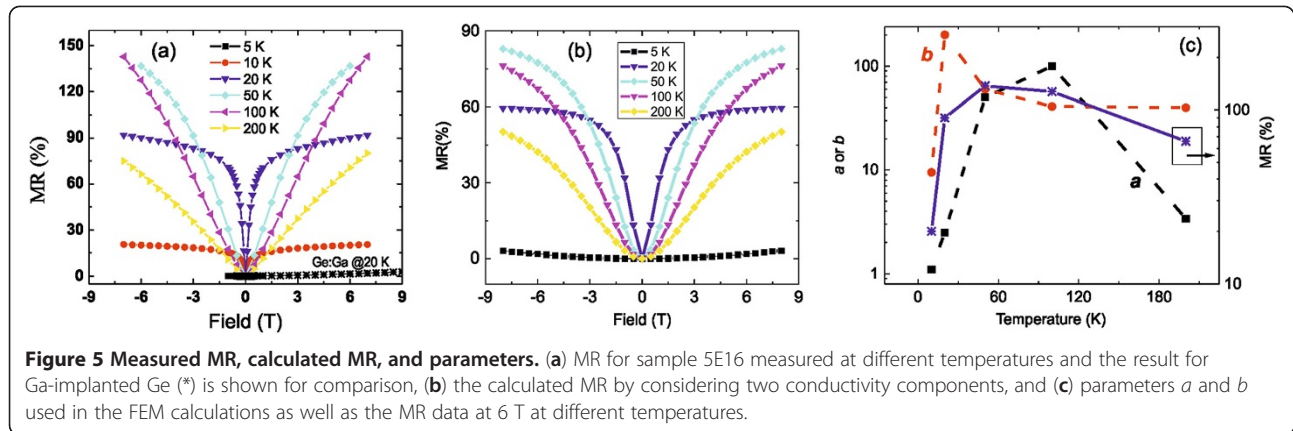


Figure 4 Mn $L_{2,3}$ X-ray absorption. (a) XAS for magnetization and helicity parallel ($\mu+$) and antiparallel ($\mu-$) and (b) XMCD ($\mu+ - \mu-$) measured at around 10 K under an external field of 6,000 Oe applied perpendicular to the surface.

Mn₅Ge₃ [28]. The XAS spectra can be classified into the $2p_{3/2}$ (approximately 641 eV) and $2p_{1/2}$ (approximately 651 eV) absorption regions. The shape of the main feature indicates the itinerant nature of ferromagnetic Mn₅Ge₃. On the other hand, the weak shoulders appear at 642 and 644 eV, and the doublet structure is observed in the $2p_{1/2}$ excitation region, which could be related with some diluted Mn impurities in the Ge matrix [21] or oxidized Mn [29]. Figure 4b shows the XMCD spectrum, revealing a large negative signal (approximately 641 eV) and a small positive signal (approximately 644 eV) in the $2p_{3/2}$ region and a larger positive signal (approximately 651.5 eV) in the $2p_{1/2}$ region. Note that the shoulders and the doublet in XAS spectra are hardly resolvable in the XMCD spectrum, which indicates that the oxidized Mn ions have no contribution to the ferromagnetism. According to the sum rule, the integrated intensity of the XMCD signal in the whole region is proportional to the orbital magnetic moment relative to the spin magnetic moment. In the present XMCD spectrum, the integration is nearly zero, indicating that the orbital magnetic moment is negligible for Mn₅Ge₃. Comparing our experimental results with the published calculations, the electronic structure of Mn ions can be assumed to be in the $3d^6$ configuration without spin-orbit interaction [28,30].

Magnetotransport properties

All three samples show p-type conductivity and large magnetoresistance (MR) effect. Figure 5a shows the



measurement results for sample 5E16. The MR is defined as $[R(H) - R(0)] / R(0)$, where $R(H)$ is the sheet resistance at a field of H , $R(0)$ is the sheet resistance at zero field. One can see that MR is positive and may saturate at a large field. Different from ferromagnetic semiconductors or metals, there is no hysteresis in MR curves for the Mn_5Ge_3/Ge hybrids. In this case, the spin scattering should have a very small contribution to transport. Similar positive MR effect has also been reported for GeMn-nanocolumns/Ge hybrids [15]. Note that the Ga-doped Ge shows only the neglectable MR effect as shown in Figure 5a. The MR effect can be interpreted by the inhomogeneity of the sample: the different conductivity and Hall resistivity of GeMn and Ge (or Mn-rich and -poor regions). We modeled the hybrid system where Mn-rich nanoparticles were embedded in the Ge matrix by a 2D slice as in the work of Yu et al. [31]. Under steady-state conditions, the continuity of the current requires that $\nabla \cdot [\sigma \cdot \nabla U(x, y)] = 0$, where $U(x, y)$ is the electrostatic potential at position (x, y) on the 2D slice. The materials were fully characterized by their conduction matrices, which vary with the position of different materials. Thus, the finite element method (FEM) proposed by Moussa et al. [32] was used. We applied a constant potential between two electrodes and calculated the induced averaged potential difference at the other two electrodes in the geometry of the van der Pauw method. The current normal to the boundary of the slice was set to zero (the natural boundary condition). The transport properties of the matrix and nanocrystal are simple, characterized by the conductivity matrix with the components:

$$\sigma_{xx}(\beta) = \sigma_{yy}(\beta) = \frac{\sigma(0)}{[1 + \beta^2]},$$

$$\sigma_{xy}(\beta) = -\sigma_{yx}(\beta) = -\frac{\sigma(0)\beta}{[1 + \beta^2]},$$

where $\sigma(0)$ is the zero-field conductivity and $\beta = R_H \sigma(0) \mu_0 H$, in which R_H is the Hall coefficient of the materials and μ_0 is the susceptibility in vacuum.

The material parameters of the matrix are chosen to be $\sigma_H^{Ge}(0) = 10^4 \Omega m^{-1}$, $R_H^{Ge} = 10^{-6} C^{-1} m^3$. The material parameters of the nanocrystal are as follows: $\sigma_H^{GeMn}(0) = a \sigma_H^{Ge}(0)$ and $R_H^{GeMn} = b R_H^{Ge}$. There are two free parameters a and b which are the ratios of conductivity and Hall coefficient of the two phases, respectively. Both the conductivity and the Hall coefficient are functions of temperature. The resistance of the system is calculated by FEM where a constant current is applied and the corresponding voltages are measured in the geometry of the van der Pauw method. The calculated curves are presented in Figure 5b. The experimental MR curves can be well reproduced by FEM calculations. The a and b values used in the FEM calculations are shown in Figure 5c. The MR magnitude is sensitive to the ratio of conductivity of the two constituents. Beside the magnetoresistance, the samples also show anomalous Hall resistance (i.e., the Hall resistance deviates from a linear behavior), which can be explained by two kinds of carriers with different mobilities [33]. On the other hand, we have to note the rather large discrepancy in the MR magnitude between the experimental and modeled values. In the model, for simplifying, we neglect the anomalous Hall effect in the GeMn constitute, which may induce this discrepancy. Also, in order to account non-monotonic dependence of MR on temperature (see Figure 5c), we have to vary parameters a and b accordingly. The decrease of a and b at temperature below 50 K cannot be understood and is the aim for the future work.

Conclusions

We have prepared magnetic Mn_5Ge_3 nanocrystals embedded inside the Ge matrix by Mn ion implantation into Ge substrates. The crystalline size of Mn_5Ge_3 can be tuned by varying the Mn fluence. The Mn ions in Mn_5Ge_3 nanocrystals are in the $3d^6$ configuration. Large

positive magnetoresistance has been observed in the $\text{Mn}_5\text{Ge}_3/\text{Ge}$ hybrid system. It could be due to the inhomogeneity in samples with constitutes having different transport properties.

Competing interests

The authors declare that they have no competing interests.

Authors' contributions

SZ designed the experiments and wrote the manuscript. WXZ and ZH made fittings for the magnetoresistance data. AS performed the XRD measurement. YW carried out the XMCD and XAS measurements. DB and HS helped during magneto-transport measurement. AM performed the TEM characterization. WLZ supervised the fitting of the magnetoresistance data. MH supervised the whole work. All authors read and approved the final manuscript.

Acknowledgments

The work was supported by the Helmholtz-Gemeinschaft Deutscher Forschungszentren (HGF-VH-NG-713) and by the International Science and Technology Cooperation Program of China (2012DFA51430). Heidemarie Schmidt thanks the financial support from DFG SCHM1663/4-1.

Author details

¹Institute of Ion Beam Physics and Materials Research, Helmholtz-Zentrum Dresden-Rossendorf, PO Box 510119, Dresden 01314, Germany. ²State Key Laboratory of Electronic Thin Films and Integrated Devices, University of Electronic Science and Technology of China, Chengdu 610054, China. ³Technische Universität Dresden, Dresden 01062, Germany. ⁴Fakultät Elektrotechnik und Informationstechnik, Materialsysteme der Nanoelektronik, Technische Universität Chemnitz, Chemnitz 09107, Germany.

Received: 14 July 2012 Accepted: 2 September 2012

Published: 25 September 2012

References

- Bihler C, Jaeger C, Vallaitis T, Gjukic M, Brandt MS, Pippel E, Woltersdorf J, Gosele U: **Structural and magnetic properties of Mn_5Ge_3 clusters in a dilute magnetic germanium matrix.** *Appl Phys Lett* 2006, **88**:112506.
- Ahlers S, Bougeard D, Sircar N, Abstreiter G, Trampert A, Opel M, Gross R: **Magnetic and structural properties of $\text{Ge}_x\text{Mn}_{1-x}$ films: precipitation of intermetallic nanomagnets.** *Physical Review B* 2006, **74**:214411.
- Passacantando M, Ottaviano L, D'Orazio F, Lucari F, De Biase M, Impellizzeri G, Priolo F: **Growth of ferromagnetic nanoparticles in a diluted magnetic semiconductor obtained by Mn^{2+} implantation on Ge single crystals.** *Physical Review B* 2006, **73**:195207.
- Wang Y, Zou J, Zhao Z, Han X, Zhou X, Wang KL: **Direct structural evidences of $\text{Mn}_{11}\text{Ge}_8$ and Mn_5Ge_2 clusters in $\text{Ge}_{0.96}\text{Mn}_{0.04}$ thin films.** *Appl Phys Lett* 2008, **92**:101913.
- Devillers T, Jamet M, Barski A, Poydenot V, Bayle-Guillemaud P, Bellet-Amalric E, Cherifi S, Cibert J: **Structure and magnetism of self-organized $\text{Ge}_{1-x}\text{Mn}_x$ nanocolumns on Ge(001).** *Physical Review B* 2007, **76**:205306.
- De Padova P, Ayoub JP, Berbezier I, Perfetti P, Quaresima C, Testa AM, Fiorani D, Olivieri B, Mariot JM, Taleb-Ibrahimi A, Richter MC, Heckmann O, Hricovini K: **$\text{Mn}_{0.06}\text{Ge}_{0.94}$ diluted magnetic semiconductor epitaxially grown on Ge(001): influence of Mn_5Ge_3 nanoscopic clusters on the electronic and magnetic properties.** *Physical Review B* 2008, **77**:045203.
- Picozzi S, Continenza A, Freeman AJ: **First-principles characterization of ferromagnetic Mn_5Ge_3 for spintronic applications.** *Physical Review B* 2004, **70**:235205.
- Jain A, Louahadj L, Peiro J, Le Breton JC, Vergnaud C, Barski A, Beigne C, Notin L, Marty A, Baltz V, Auffret S, Augendre E, Jaffrès H, George JM, Jamet M: **Electrical spin injection and detection at $\text{Al}_2\text{O}_3/\text{n-type germanium}$ interface using three terminal geometry.** *Appl Phys Lett* 2011, **99**:162102–162103.
- Jain A, Vergnaud C, Peiro J, Le Breton JC, Prestat E, Louahadj L, Portemont C, Ducruet C, Baltz V, Marty A, Barski A, Bayle-Guillemaud P, Vila L, Attané JP, Augendre E, Jaffrès H, George JM, Jamet M: **Electrical and thermal spin accumulation in germanium.** *Appl Phys Lett* 2012, **101**:022402–022404.
- Zeng C, Erwin SC, Feldman LC, Li AP, Jin R, Song Y, Thompson JR, Weitering HH: **Epitaxial ferromagnetic Mn_5Ge_3 on Ge(111).** *Appl Phys Lett* 2003, **83**:5002–5004.
- Zeng C, Yao Y, Niu Q, Weitering HH: **Linear magnetization dependence of the intrinsic anomalous Hall effect.** *Phys Rev Lett* 2006, **96**:037204.
- Kim H, Jung G-E, Lim J-H, Chung KH, Kahng S-J, Son W-j, Han S: **Epitaxial Mn_5Ge_3 nano-islands on a Ge(001) surface.** *Nanotechnology* 2008, **19**:025707.
- Spießner A, Slipukhina I, Dau MT, Arras E, Le Thanh V, Michez L, Pochet P, Saito H, Yuasa S, Jamet M, Derrien J: **Control of magnetic properties of epitaxial $\text{Mn}_5\text{Ge}_3\text{C}_x$ films induced by carbon doping.** *Physical Review B* 2011, **84**:165203.
- Jain A, Jamet M, Barski A, Devillers T, Porret C, Bayle-Guillemaud P, Gambarelli S, Maurel V, Desfonds G: **Investigation of magnetic anisotropy of (Ge, Mn) nanocolumns.** *Appl Phys Lett* 2010, **97**:202502–202503.
- Jamet M, Barski A, Devillers T, Poydenot V, Du Jardin R, Bayle-Guillemaud P, Rothman J, Bellet-Amalric E, Marty A, Cibert J, Mattana R, Tatarenko S: **High-Curie-temperature ferromagnetism in self-organized $\text{Ge}_{1-x}\text{Mn}_x$ nanocolumns.** *Nat Mater* 2006, **5**:653–659.
- Bougeard D, Ahlers S, Trampert A, Sircar N, Abstreiter G: **Clustering in a precipitate-free GeMn magnetic semiconductor.** *Phys Rev Lett* 2006, **97**:237202.
- Li AP, Zeng C, van Benthem K, Chisholm MF, Shen J, Nageswara Rao SVS, Dixit SK, Feldman LC, Petukhov AG, Foygel M, Weitering HH: **Dopant segregation and giant magnetoresistance in manganese-doped germanium.** *Physical Review B* 2007, **75**:201201.
- Xiu F, Wang Y, Kim J, Hong A, Tang J, Jacob AP, Zou J, Wang KL: **Electric-field-controlled ferromagnetism in high-Curie-temperature $\text{Mn}_{0.05}\text{Ge}_{0.95}$ quantum dots.** *Nat Mater* 2010, **9**:337–344.
- Wang Y, Xiu FX, Zou J, Beyermann WP, Zhou Y, Wang KL: **Coherent magnetic semiconductor nanodot arrays.** *Nanoscale Res Lett* 2011, **6**:134.
- Ottaviano L, Passacantando M, Picozzi S, Continenza A, Gunnella R, Verna A, Bihlmayer G, Impellizzeri G, Priolo F: **Phase separation and dilution in implanted $\text{Mn}_x\text{Ge}_{1-x}$ alloys.** *Appl Phys Lett* 2006, **88**:061907.
- Ottaviano L, Passacantando M, Verna A, D'Amico F, Gunnella R: **Mn $L_{2,3}$ x-ray absorption spectra of a diluted Mn-Ge alloy.** *Appl Phys Lett* 2007, **90**:242105.
- Zhou S, Shalimov A, Potzger K, Jeutter NM, Baehtz C, Helm M, Fassbender J, Schmidt H: **Memory effect of Mn_5Ge_3 nanomagnets embedded inside a Mn-diluted Ge matrix.** *Appl Phys Lett* 2009, **95**:192505.
- Zhou S, Burger D, Skorupa W, Oesterlin P, Helm M, Schmidt H: **The importance of hole concentration in establishing carrier-mediated ferromagnetism in Mn doped Ge.** *Appl Phys Lett* 2010, **96**:202105.
- Burger D, Zhou S, Howler M, Ou X, Kovacs GJ, Reuther H, Mücklich A, Skorupa W, Helm M, Schmidt H: **Hysteretic anomalous Hall effect in a ferromagnetic Mn-rich Ge/Mn nanonet.** *Appl Phys Lett* 2012, **100**:012406.
- Surgers C, Potzger K, Strache T, Moller W, Fischer G, Joshi N, Lohneysen H: **Magnetic order by C-ion implantation into Mn_5Si_3 and Mn_5Ge_3 and its lateral modification.** *Appl Phys Lett* 2008, **93**:062503.
- Jain A, Jamet M, Barski A, Devillers T, Yu IS, Porret C, Bayle-Guillemaud P, Favre-Nicolin V, Gambarelli S, Maurel V, Desfonds G, Jacquot JF, Tardif S: **Structure and magnetism of Ge_3Mn_5 clusters.** *J Appl Phys* 2011, **109**:013911–013914.
- Ahlers S, Stone PR, Sircar N, Arenholz E, Dubon OD, Bougeard D: **Comparison of the magnetic properties of GeMn thin films through Mn L-edge x-ray absorption.** *Appl Phys Lett* 2009, **95**:151911.
- Hirai C, Sato H, Kimura A, Yaji K, Iori K, Taniguchi M, Hiraoka K, Muro T, Tanaka A: **Mn 2p–3d soft X-ray magnetic circular dichroism study of Mn_5Ge_3 .** *Physica B* 2004, **351**:341–343.
- Tardif S, Cherifi S, Jamet M, Devillers T, Barski A, Schmitz D, Darowski N, Thakur P, Cezar JC, Brookes NB, Mattana R, Cibert J: **Exchange bias in GeMn nanocolumns: the role of surface oxidation.** *Appl Phys Lett* 2010, **97**:062501–062503.
- Sangaletti L, Drera G, Magnano E, Bondino F, Cepek C, Sepe A, Goldoni A: **Atomic approach to core-level spectroscopy of delocalized systems: case of ferromagnetic metallic Mn_5Ge_3 .** *Physical Review B* 2010, **81**:085204.

31. Yu I-S, Jamet M, Marty A, Devillers T, Barski A, Beigne C, Bayle-Guillemaud P, Cibert J: **Modeling magnetotransport in inhomogeneous (Ge, Mn) films.** *J Appl Phys* 2011, **109**:123906.
32. Moussa J, Ram-Mohan LR, Sullivan J, Zhou T, Hines DR, Solin SA: **Finite-element modeling of extraordinary magnetoresistance in thin film semiconductors with metallic inclusions.** *Physical Review B* 2001, **64**:184410.
33. Zhou S, Burger D, Helm M, Schmidt H: **Anomalous Hall resistance in Ge: Mn systems with low Mn concentrations.** *Appl Phys Lett* 2009, **95**:172103.

doi:10.1186/1556-276X-7-528

Cite this article as: Zhou et al.: Magnetic Mn₅Ge₃ nanocrystals embedded in crystalline Ge: a magnet/semiconductor hybrid synthesized by ion implantation. *Nanoscale Research Letters* 2012 **7**:528.

Submit your manuscript to a SpringerOpen[®] journal and benefit from:

- ▶ Convenient online submission
- ▶ Rigorous peer review
- ▶ Immediate publication on acceptance
- ▶ Open access: articles freely available online
- ▶ High visibility within the field
- ▶ Retaining the copyright to your article

Submit your next manuscript at ▶ springeropen.com
